Advanced Atmospheric Mitigation Decision Aids for Space Imaging and Laser Communications

Randall J. Alliss, Heather Kiley, Mary Ellen Craddock, Danny Felton, Michael Mason

Northrop Grumman Mission Systems
7555 Colshire Dr
McLean, VA 22102

Abstract

Space based imaging often times wastes its onboard resources capturing pictures of the tops of clouds when ground targeting could be easily optimized with the use of atmospheric mitigation decision aids. The interest in the use of space based optical communications, also known as laser communications, is also similarly impacted by clouds and could benefit from similar atmospheric mitigation decision aids in order to optimize its link availability. Laser communications provide secure, high data rate transmission in the absence of strong atmospheric fading that includes cloud liquid water, ice and atmospheric aberrations produced by pancake layer density gradients. A multi-year campaign to understand the impacts of atmospherics on space imaging as well as laser communication signals is underway. This campaign includes quantifying the impacts of the atmosphere on atmospheric data links, and developing operational concepts for mitigating transmission losses due to clouds, turbulence, and aerosols.

Advanced atmospheric mitigation decision aids for characterizing and forecasting optical links and for optimizing resources for ground imaging is currently being developed. They include the development and deployment of state of the art instruments designed to measure properties of clouds, including transmission loss, at optical ground sites. An Infrared Cloud Imager and LIDAR ceilometer will together provide high temporal frequency characterization of clouds and cloud transmission in the local skydome. This data will provide an estimate of the atmospheric fading and will be used to make decisions on switching the link from one optical ground site to another. In addition to *in situ* measurements of clouds, remote sensing geostationary satellites will provide improved resolution of clouds in and near the site as well as regionally around each site in the optical network. Finally, combined use of numerical prediction of atmospherics including cloud and optical turbulence fading and artificial intelligence are underway and will help to optimize ground target resourcing hours and days in advance. Combining local and regional characterization along with high fidelity numerical modeling and deep machine learning is resulting in an optimized atmospheric mitigation decision aid that maximizes availability.

1. INTRODUCTION

With ever-increasing amounts of space-based data being generated and transmitted by commercial, government and military, modern society is increasingly reliant on high-performance and secure satellite communications. As users continue to demand more data, the existing communications infrastructure will have to expand to meet the demands. Radio Frequency signals have been relied on exclusively and successfully to communicate with spacecraft since satellite communications began nearly 60 years ago, but there are limitations that may prevent radio frequency communications from fully meeting future requirements. These technical, regulatory, and financial limitations may be alleviated, in part, by Free-Space Optical Communications (FSOC). There are several advantages to using FSOC to meet future communications requirements. In particular, data can be transmitted through free-space via lasers at very high data rates of multi-Gb/s over long distances. Optical beams are also very narrow making them much less susceptible to jamming than radio frequency signals. Additionally, unlike radio frequencies, the optical spectrum is currently unregulated. Finally, optical communications systems are relatively small and potentially much less expensive than comparable radio frequency systems, particularly for air and space missions.

The ultimate realization of practical, high-availability FSOC systems, however, will depend on how well they can mitigate the impacts of atmospheric effects, primarily cloud cover and optical turbulence (OT). Clouds are the largest source of atmospheric attenuation for space-to-ground optical communications, often producing transmission losses of several decibels (dBs) to several tens of dBs. Without impractically large link margins, most clouds are generally considered blockages to FSOC links.

Since atmospheric phenomena such as clouds are the major limiting factor to the success of FSOC, ground sites for FSOC systems are preferentially located in areas with little to no atmospheric interference (i.e. dry and largely cloud-free sites). One such location is the Haleakala summit on the Hawaiian island of Maui where a semi-persistent low-level temperature inversion often traps clouds below the summit. Due to its favorable atmospherics Haleakala and Table Mountain Facility in Southern California are optical ground sites for NASA's upcoming Laser Communication Relay Demonstration (LCRD).

A unique opportunity exists at both sites to collect first ever measurements of atmospheric losses associated specifically with clouds. An array of instrumentation has recently been deployed to quantify optical impacts. This paper summarizes efforts to date taken to characterize Haleakala. Section two describes the instrumentation deployed. Section three shows analysis to date of some of the parameters collected. Section four shows how a machine learning algorithm is being utilized to make shortterm predictions of cloud cover. A summary of the results and future directions are provided in Section 5.

2. INSTRUMENTS

Figure 1 shows the Atmospheric Monitoring Station (AMS) at NASA's Optical Ground Station – 2 (OGS2). The AMS consists of three main instrumentation, the Vaisala AWS 310 which measures temperature, pressure, wind speed direction, humidity, rain, and incoming solar radiation, the Vasiala Ceilometer 51 (CL51) which measures backscatter off of aerosols and clouds and the Infrared Cloud Imager (ICI). The AMS was deployed in 2017 with approximately 13 months of data collected as of this writing.

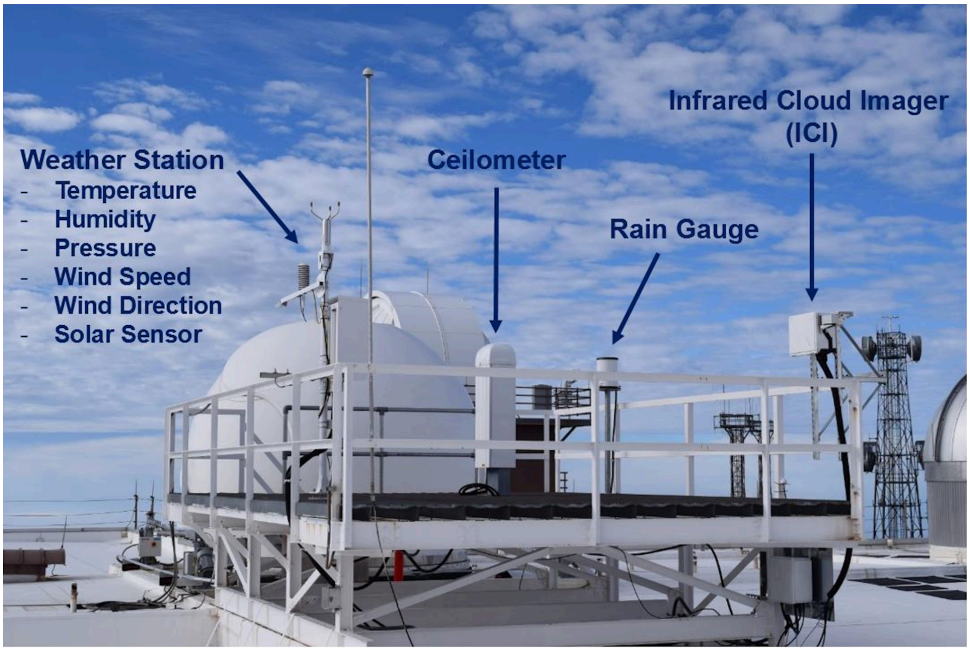

Figure 1. The Atmospheric Monitoring Station (AMS) at Haleakala, HI.

a. AWS310

The Vaisala Automatic Weather Station (AWS) is a standalone weather station that measures air temperature, humidity, pressure, wind speed and direction, precipitation amount and incoming solar radiation. The system runs autonomously collecting these parameters at sub 1 minute intervals. Data is ingested and archived for analysis on a combination of windows and linux workstations. A pyranometer was also deployed to measure incoming solar radiation and to estimate the transmission loss due to clouds during the daytime.

b. CL51

The Vaisala Ceilometer CL51 employs pulsed diode laser LIDAR technology, where short, powerful laser pulses are sent out in a vertical direction. The reflection of light, backscatter – caused by haze, fog, mist, precipitation, and clouds - is measured as the laser pulses traverse the vertical column above the site. The resulting backscatter profile, which is a measure of intensity as a function of height, is stored and processed at six second intervals to compute cloud base heights and transmission loss. The time it takes between the launch of the laser pulse and the detection of the backscatter signal defines the cloud base height. Backscatter profiles are available up to approximately 16 kilometers above ground level. Figure 2 shows an example of a time series of filtered backscatter. The cloud base in this case ranges between 2500 and 3000 meters above ground.

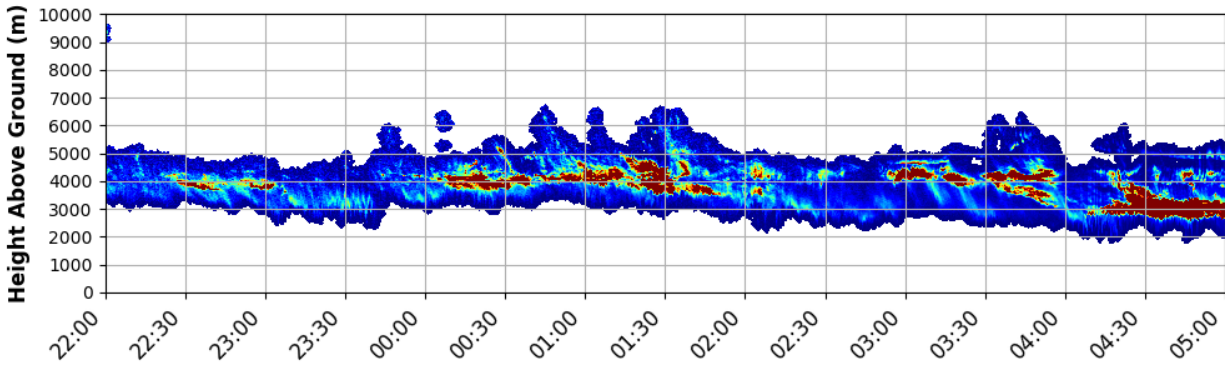

Figure 2. Seven hour time series of backscatter from the CL51 instrument. Larger returns are associated with more concentrated cloud droplets.

c. *Infrared Cloud Imager (ICI)*

The Infrared Cloud Imager (ICI) uses a FLIR Photon 640 camera mounted underneath a stingray full sky lens. Figure 3 shows the ICI system which consists of a camera and electronics (not shown) enclosure, respectively. The ICI system was designed to capture calibrated IR images at up to 20 second intervals with the ability to shut down in the presence of rain in order to prevent water droplets from collecting on the stingray lens. The shutdown procedure is initiated by the presence of a rain sensor which when triggered by any rain drops sends a signal to the hatch to close over top the lens. Only after the rain sensor no longer detects drops does the hatch re-open and image collection resumes. The ICI has the benefit of being able to collect images day/night in the presence of sun and moonlight. The images are stored as calibrated radiances with units of Watts/m^2/steradian. Example images under a variety of conditions are shown in Figure 4. A cloud retrieval algorithm has been developed to interpret each image at the pixel level as cloud or no cloud. This algorithm uses the clear sky background (CSB) technique [1] which evaluates many sky radiance images as a function of time of day and identifies the 10th percentile lowest values. The 10th percentile is typically associated with an image absent of observable clouds based on coincident observations from the CL51. A given image is then compared to the current CSB and if the difference is more than 0.5 Watts then the pixel is labeled cloudy. Conversely, a machine learning algorithm composed of a recurrent convolutional neural network (RCNN) is employed on an nvidia P100 graphical processing unit (GPU). The RCNN trains on thousands of ICI sky radiances to produce a model that then predicts cloud no cloud at each pixel. Both methods produce very similar results. In addition, an algorithm currently under development, assigns an atmospheric transmission loss to each pixel.

Figure 3. The infrared Cloud Imager (ICI) located above the clouds on the summit (10,000 feet AMSL) of Haleakala, HI.

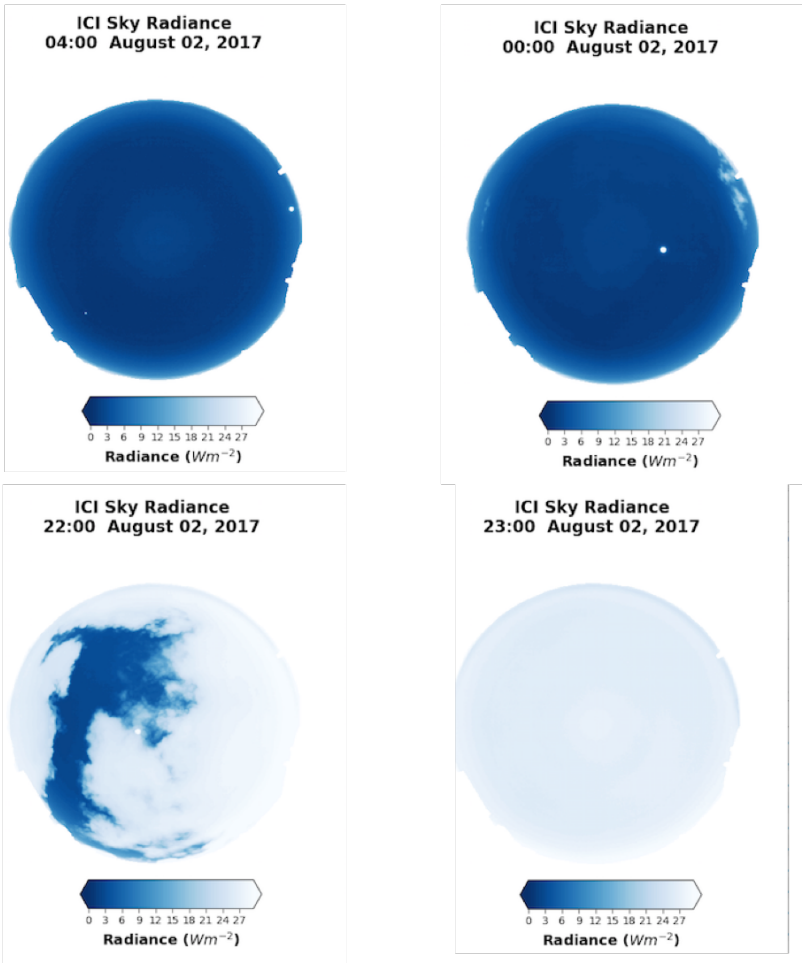

Figure 4. Example ICI sky radiance images (W/m2/sr). Low values of sky radiances are consistent with clear skies while large values are associated with varying thickness of clouds.

3. ANALYSIS OF DATA

Since this study is most interested in the impact of clouds on optical communications it makes sense to describe the climatology of clouds at Haleakala, HI. A high resolution cloud database has been developed [2] over the Hawaiian Islands. The database is based on 4km horizontal resolution visible and infrared imagery collected from the various NOAA GOES satellites and run through a cloud retrieval algorithm. Data from 1997 – 2018 has been processed so that FSOC applications can be investigated. Figure 5 shows a climatology of the Cloud Free Line of Sight (CFLOS) also known as "Availability" for Haleakala as a function of month of the year. Both the mean CFLOS (blue x's) and the individual months availability (red dots) are shown in order to present the intra-annual variability. The green stars indicate the availability for the months between July 2017 and April 2018 as indicated by the Satellite retrievals. This period is highlighted to inter compare with a similar estimate derived from the ICI cloud retrievals. These retrievals are shown by the black diamonds from August 2017 through April 2018. The mean availability of this site is approximately 72% but with a mean range of 59 to 82%. The red dots indicate that over the last 21 years considerable variability exists and in fact one of the cloudiness periods on record was observed earlier in 2018. Although the satellite record indicates very low availabilities as compared to its own data, the corresponding ICI data indicates even lower availabilities with a low of 25% in April of this year. The difference

between the ICI and the satellite estimates may be associated with the much higher spatial resolution of the ICI as well as the increased sensitivity in thin clouds as compared to the satellite. In August and September of 2017 the ICI actually shows fewer clouds as compared to the satellite and we believe this is associated with the superior horizontal resolution of the ICI compared with the 4km footprint of GOES which can barely resolve the summit of Haleakala.

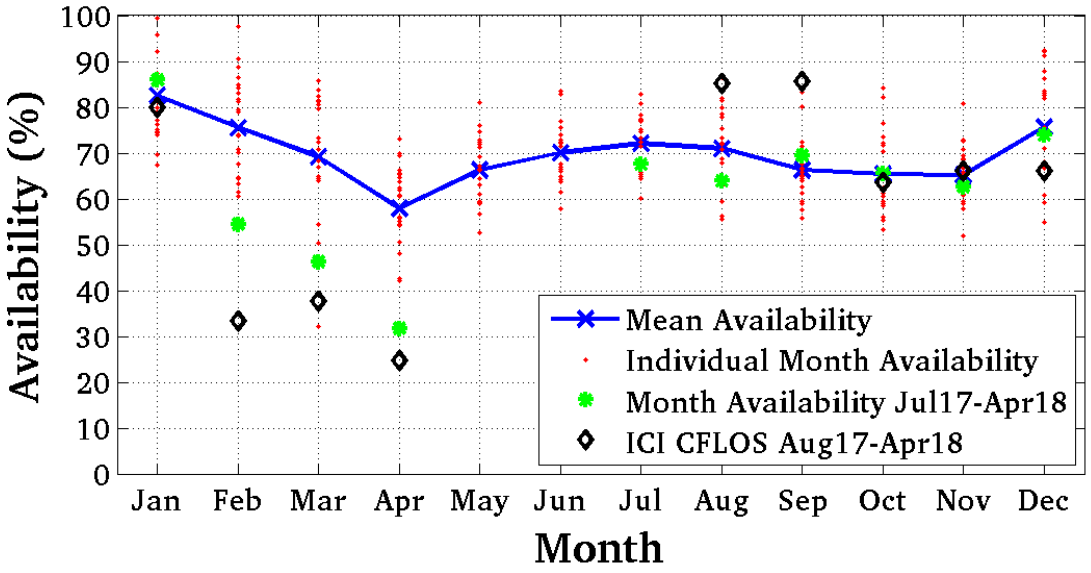

Figure 5. Climatology of Availability at Haleakala, HI based on 21 years of GOES imagery.

As indicated above, the AWS310 captures one minute resolution temperature, humidity and wind speed information. These parameters are important to FSOC because of their impact on various dome operations associated with the ground terminal. Figure 6abc shows a cumulative distribution of temperature, relative humidity and wind speed. The median temperature is approximately 8C but the probability that the site drops below freezing is far less than 1%. However, an observed snowfall accumulation was reported at the summit during the winter of 2018. As one would expect at a 10,000 foot summit, the observed relative humidity is quite low most of the time. Saturated conditions were only observed approximately 20% of the time in the past year. This parameter is important to monitor in order to prevent the optical window from becoming coated with either rain or condensation.

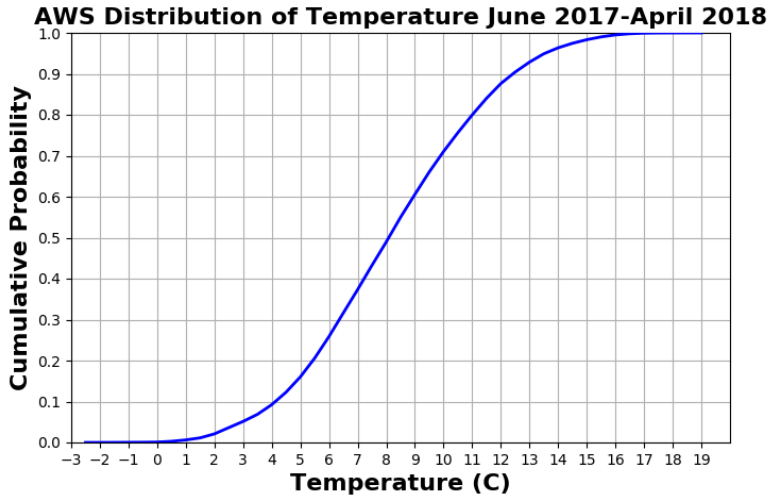

Figure 6a CDF of temperature at Haleakala, HI.

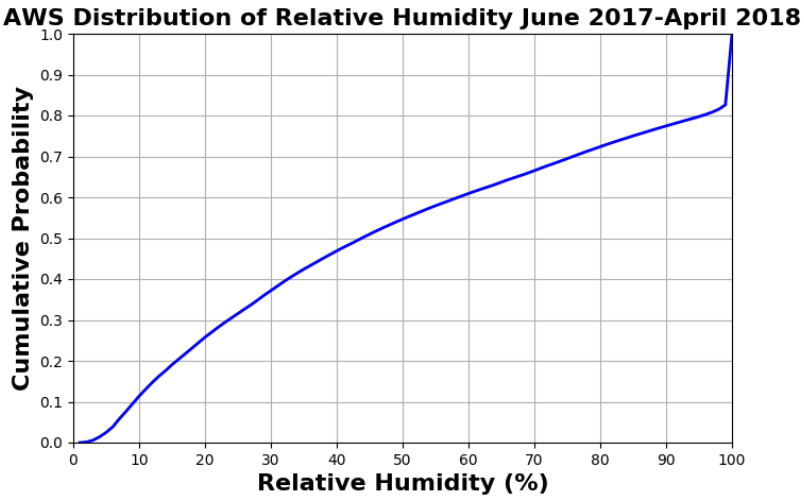

Figure 6b. CDF of relative humidity. Saturated conditions only observed 20% of the time.

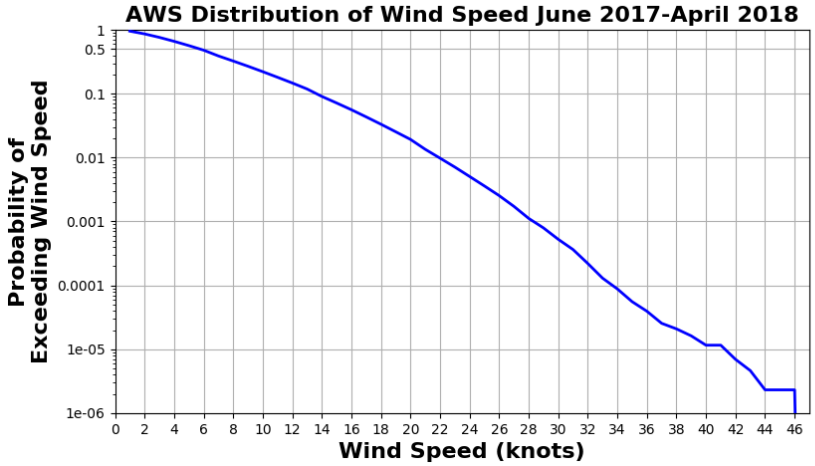

Figure 6c. CDF of surface wind speed. High winds were rarely observed.

Winds at the summit are also another factor for dome operations. Depending on the dome ratings winds could cause the site to be unavailable. In the last year, however, winds were not a factor with the median wind well below 10knts and the greatest wind observed not more than approximately 45 knts.

An estimate of the transmission loss due to clouds was made using data collected from the pyranometer. The technique uses the ratio of measured incoming solar insolation to that of the theoretical incoming in the absence of clouds and aerosols for this site. Estimates were limited to times when the solar elevation angle was greater than 20 degrees. Figure 7 shows the distribution of transmission loss, expressed in dB fade, for the site during the last year. The median fade was approximately 3dB which is consistent with what has been observed from the Mees observatory observations of the same parameter over the last four years. This may have significant implications for FSOC as any link budget who factors in just a few dB for clouds could greatly increase site availability and ultimately how much data could be transmitted to the ground even in the presence of thin clouds. An inner comparison with the CL51 and ICI are currently being performed to increase confidence in these results.

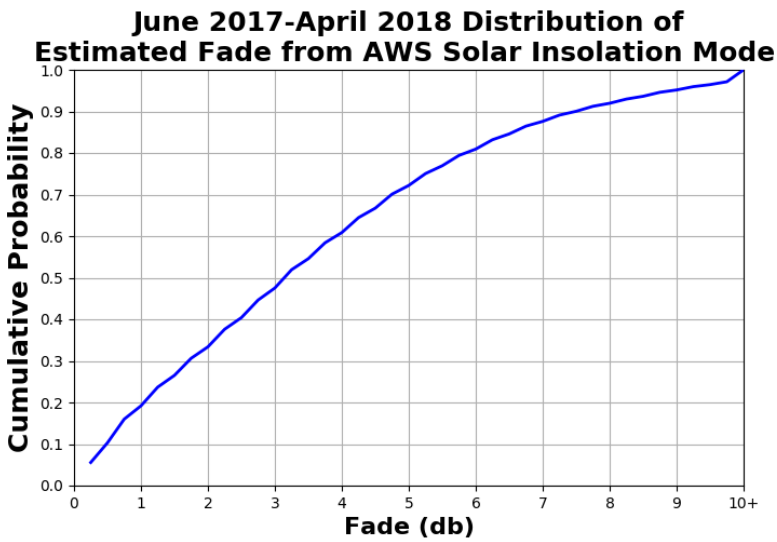

Figure 7. Distribution of fade derived from the pyranometer. The median attenuation of clouds observed is approximately 3dB.

4. SHORT-TERM PREDICTIONS

The ML technique demonstrated here is an ensemble learning method called Random Forest [3]. Random Forest (RF) is a powerful non-linear statistical analysis approach that has been shown to offer advantages in many different environmental realms. RF has proven applicable to a variety of problems from predicting clouds using a numerical model [4,5], cloud detection from satellite [6], atmospheric turbulence [7] to determining flood hazard risk [8]. RFs are ensembles of weakly-correlated and weak-learning decision trees that each vote on a single outcome. The overall result of a RF model can be either a binary classification of an outcome based on the majority vote from all the trees in the forest or a probability of an outcome based on the distribution of the votes within the forest. For the purposes of this project, the former binary classification approach is implemented.

For each tree in the random forest, a random subset (usually about 2/3) of the total number of samples is drawn with replacement from a "training" dataset that consists of predictor variables and associated "truth" values. The remaining portion (usually about 1/3) of the total number of samples is used to evaluate the unbiased mean square error (a.k.a. out-of-bag, OOB error) of the resulting decision tree model. At each node of the tree, a random *mtry* number of the input predictor variables are chosen which provides candidates for splitting the data. The data is split into two parts based on a condition/value of a single predictor variable (a.k.a "feature") such that similar samples end up in the same set. The measure based on which the locally optimal condition is chosen is called the Gini impurity index, which indicates how often a randomly chose sample from a set of data would be incorrectly labeled if it were labeled according to the distribution of labels within the dataset. The degree to which each feature decreases the weighted Gini impurity among the various trees in the forest (a.k.a. "feature importance") is recorded through this process.

The goal of this effort is to take sequential images of ICI cloud no cloud retrievals and predict the probability of clouds at various time intervals [1,2,3,5,10,15 min] into the future. Afterwards, a cloud "outage" risk assessment is then developed based on the predictions. The Random Forest requires predictors used for this study are shown in Figure 8. The skydome cloud amount from the entire ICI image, the cloud determination for the line of sight (red star), the cloud amounts for the inner/outer (10° and 20°) rings and their time averaged and standard deviations are used as predictors. The model is trained on one minute images obtained from August and September 2017. The feature importance's for the five minute training model are shown in Figure 9. The top three predictors in this case are the most recent 20° ring cloud fraction, the total image cloud fraction and inner 10° ring cloud fraction.

To quantify the accuracy of the model, predictions out to 15 minutes are made for an independent period from October 2017 – February 2018. Contingency tables are developed that compare the predictions to the ICI "truth" which in this case are the cloud masks derived from the algorithm presented in section 2c. Output of the contingency

tables are presented on a standard Roebber plot [9] which shows Probability of Detection, False Alarm Rate, bias and critical skills index (CSI).

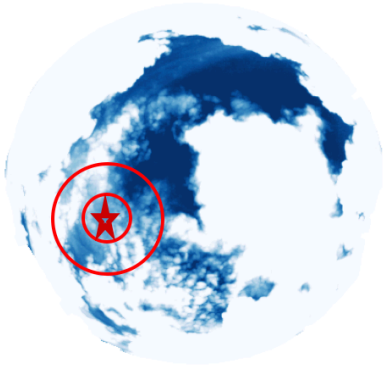

Figure 8. ICI image with predictors over layed. Cloud amount for skydome, line of sight (star), inner ring and outer ring.

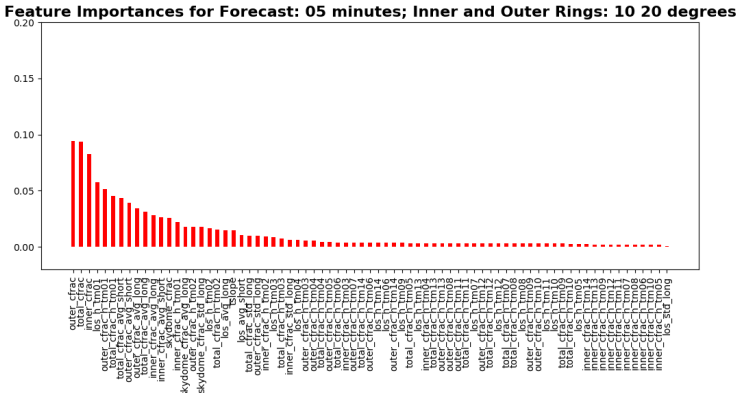

Figure 9. Feature importance's for the 5 minute training case.

Results of the random forest cloud predictions are shown in Figure 10 a. Figure 10b shows the same length forecasts but using a persistence approach so as to compare to the random forest forecasts. Persistence by definition predicts no change and therefore we would expect that any intelligent forecast would easily outperform it.

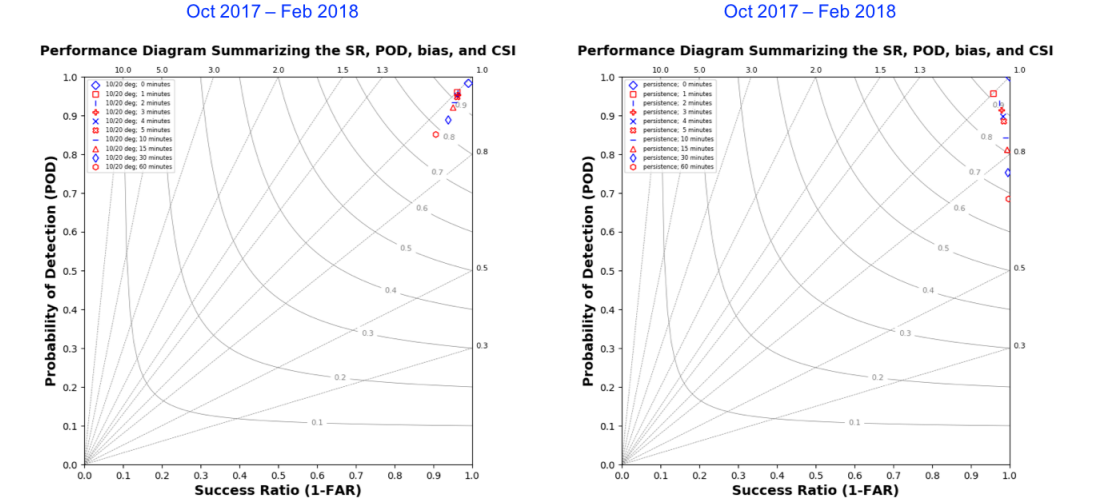

Figure 10. Roebber plots showing random forest predictions versus persistence predictions.

Results indicate that the random forest (RF) models out to 60 minutes outperform the persistence forecasts. Very little bias exists with the RF forecasts relative to the persistence and mean POD's exceed 90% out to 15 minutes. Conversely the persistence forecast has an extreme clear bias which is to be expected for such a clear location. This work is being extended to train on additional data in hopes to improve the predictions further.

5. CONCLUSION AND DISCUSSION

This study has shown the value in the development and deployment of atmospheric characterization instrumentation to sample the atmosphere at very high temporal and spatial resolution. A state of the art system was deployed to Haleakala, HI and includes an AWS310, CL51 and Infrared Cloud Imager. These instruments have been autonomously collecting data since 2017 and continue today. This capability is showing for the first time that the derivation of atmospheric attenuation due to clouds is possible and can be used to characterize the atmosphere during optical communications other EO/IR applications. Several artificial intelligence algorithms have been developed to predict the future state of the atmosphere using this data. The algorithm when evaluated on an independent period of record beats a persistence forecast out to 60 minutes. Results show much promise and additional development is planned including training models using GPU's to predict clouds.

References

[1] Alliss, R.J., and B.W. Felton: "The mitigation of Cloud Impacts on Free Space Optical Communications", SPIE Proceedings, Vol. 8380, 83819 (2012).

[2] Alliss, R.J, and B.W. Felton: "Characterization of Atmospherics in Hawaii for Space Based Optical Communications", International Conference on Space Optical Systems and Applications (ICSOS) Proceedings, 2015.

[3] Breiman, L., Random forests. *Machine Learning*, Vol. 45, 5–32, 2001.

[4] Russell, A.M, Alliss, R.J., and B.W. Felton: "A deep machine learning algorithm to optimize the forecast of atmospherics", *Advanced Maui Optical and Space Surveillance Technologies Conference*, 2017.

[5] Russell, A.M, and R.J. Alliss "Machine Learning with Numerical Weather Prediction Cloud Forecasts for Optical Communications Support" 25th Proceedings from Artificial Intelligence Symposium, American Meteorological Society, 2018.

[6] Craddock, M.E., Alliss, R.J., and M.L. Mason: "Improving the accuracy of cloud detection using machine learning", 25th Proceedings from Artificial Intelligence Symposium, American Meteorological Society, 2018.

[7] Mecikalaski, J.R., J.K. Williams, C.P, Jewett, D. Ahijevych, A. LeRoy and J.R. Walker, Probabilistic 0–1-h Convective Initiation Nowcasts that Combine Geostationary Satellite Observations and Numerical Weather Prediction Model Data, *Journal of Applied Meteorology and Climatology*, Vol. 54, 139–159, 2015.

[8] Gala, Y., A. Fernandez, J. Diaz and J.R. Dorronsoro, Hybrid machine learning forecasting of solar radiation values, *Neurocomputing*, Vol 176, 48–59, 2016.

[9] Roebber, P.J., Visualizing Multiple Measure of Forecast Quality, *Weather and Forecasting*, Vol. 24, 601–608, 2009.